The Journal of Experimental Biology 207, 2991-3002
Published by The Company of Biologists 2004
doi:10.1242/jeb.01101

Characterization and expression of plasma membrane Ca^{2+} ATPase (PMCA3) in the crayfish *Procambarus clarkii* antennal gland during molting

Yongping Gao and Michele G. Wheatly*
Department of Biological Sciences, Wright State University, Dayton, OH 45435, USA
*Author for correspondence (e-mail: michele.wheatly@wright.edu)

Accepted 18 May 2004

Summary

The discontinuous pattern of crustacean cuticular mineralization (the molting cycle) has emerged as a model system to study the spatial and temporal regulation of genes that code for Ca^{2+}-transporting proteins including pumps, channels and exchangers. The plasma membrane Ca^{2+}-ATPase (PMCA) is potentially of significant interest due to its role in the active transport of Ca^{2+} across the basolateral membrane, which is required for routine maintenance of intracellular Ca^{2+} as well as unidirectional Ca^{2+} influx. Prior research has suggested that PMCA expression is upregulated during periods of elevated Ca^{2+} influx associated with postmolt cuticular mineralization. This paper describes the cloning, sequencing and functional characterization of a novel *PMCA3* gene from the antennal gland (kidney) of the crayfish *Procambarus clarkii.* The complete sequence, the first obtained from a non-genetic invertebrate species, was obtained through reverse transcription-polymerase chain reaction (RT-PCR) and rapid amplification of cDNA ends (RACE) techniques. Crayfish *PMCA3* consists of 4148 bp with a 3546 bp open reading frame coding for 1182 amino acid residues with a molecular mass of 130 kDa. It exhibits 77.5–80.9% identity at the mRNA level and 85.3–86.9% identity at the protein level with PMCA3 from human, mouse and rat. Membrane topography was typical of published mammalian PMCAs. Northern blot analysis of total RNA from crayfish gill, antennal gland, cardiac muscle and axial abdominal muscle revealed that a 7.5 kb species was ubiquitous. The level of *PMCA3* mRNA expression in all tissues (transporting epithelia and muscle) increased significantly in pre/postmolt stages compared with relatively low abundance in intermolt. Western analysis confirmed corresponding changes in PMCA protein expression (130 kDa).

Key words: calcium transport, plasma membrane calcium ATPase, PMCA, crayfish, *Procambarus clarkii*, antennal gland, gill, axial abdominal muscle, cardiac muscle.

Introduction

Intracellular Ca^{2+} homeostasis is critical to eukaryotic cells due to the important role that cytoplasmic free Ca^{2+} plays as a second messenger in initiating routine cellular events including excitation–contraction coupling, hormonal release, alterations in cell metabolism and growth. In general, cells attempt to keep intracellular (IC) Ca^{2+} low to preserve its function as a signaling agent and to avoid cell toxicity. Studies suggest that this involves coordination between transmembrane proteins on apical, basolateral and internal [sarco/endoplasmic reticular (SER)] membranes that import and export Ca^{2+}, such as channels, pumps, exchangers and binding proteins. Regulation of IC Ca^{2+} is further challenged in polarized epithelial cells that vectorially transfer large amounts of Ca^{2+} either in absorptive or secretory mode.

The natural molting cycle of a freshwater crayfish, *Procambarus clarkii*, has emerged as an ideal non-mammalian model to study Ca^{2+} homeostasis and the genes encoding the Ca^{2+} handling proteins (Wheatly, 1999). As arthropods, crustaceans possess an external calcified cuticle that is periodically shed, enabling growth to occur. These episodes are preceded in premolt by reabsorption of Ca^{2+} from the existing cuticle and deposition in storage sites (often regions of the digestive tract). Following ecdysis, there is intense pressure in postmolt to remineralize the new cuticle primarily with Ca^{2+} absorbed from the external water. After calcification is completed, the animal returns to intermolt, a period during which net Ca^{2+} flux is minimal. The beauty of this model system is that net Ca^{2+} flux alternates from Ca^{2+} balance (intermolt) to net loss (premolt) and then to significant net uptake (postmolt), offering an ideal model to examine the temporal and spatial regulation of genes coding for Ca^{2+} handling proteins. Among crustaceans, the crayfish exhibits highly developed strategies for Ca^{2+} homeostasis that have enabled it to evolve in freshwater, a highly inhospitable environment with respect to Ca^{2+} availability (levels typically below 1 mmol l^{-1} compared with 10 mmol l^{-1} in seawater). Specifically, the antennal gland (kidney analog) produces a dilute urine, contributing significantly to the organism's ability to maintain its hemolymph Ca^{2+} hyperionic to the external environment. This ability is relatively rare in the animal kingdom. In postmolt, the gills effect massive net Ca^{2+} influx from low external levels using active influx mechanisms.

While our lab has had a long-term interest in several Ca^{2+} import/export proteins, the most interesting and elusive of these is the high-affinity plasma membrane Ca^{2+} ATPase (PMCA) that moves Ca^{2+} against its electrochemical gradient from the cytosol into the hemolymph using hydrolysis of ATP. This protein is critical to routine maintenance of IC Ca^{2+} concentration and may have an enhanced role in transcellular Ca^{2+} influx. Physiological examination of ATP-dependent uptake into inside-out basolateral vesicles (Wheatly et al., 1999) suggests that postmolt Ca^{2+} influx at the antennal gland would necessitate proliferation of Ca^{2+} pumps, while gills appear to be engineered with an overcapacity to pump Ca^{2+}.

Initial attempts to clone Ca^{2+} pumps in crustaceans were focused on a related export protein, the sarco/endoplasmic reticulum Ca^{2+} ATPase (SERCA), which sequesters cytosolic Ca^{2+} into the SER. In crayfish, SERCA expression is highest in intermolt and decreases in pre- and postmolt in both Ca^{2+}-transporting epithelia (hepatopancreas; Y.G. and M.G.W., unpublished observations) and non-Ca^{2+}-transporting tissues alike (axial and cardiac muscle; Zhang et al., 2000; Chen et al., 2002). However, in the mineralizing anterior sternal epithelium (ASE) of the terrestrial isopod *Porcellio scaber*, upregulation of SERCA was associated with Ca^{2+}-transporting stages (late premolt and intramolt), an effect that was not apparent in nervous tissue (Hagedorn and Ziegler, 2002; Hagedorn et al., 2003).

PMCAs and SERCAs belong to the family of P-type ATPases characterized by the formation of a covalently phosphorylated obligatory intermediate that arises from the transfer of the γ phosphate of ATP to a specific aspartate residue at the catalytic site of the polypeptide during the reaction cycle; both are integral membrane proteins of 1000 amino acid residues with three cytoplasmic domains joined to a set of 10 transmembrane (TM) α helices by a narrow pentahelical stalk of α helices. PMCAs are distinguished from other P-type ATPases by their higher molecular mass (135 kDa) and the presence of a C-terminal regulatory region containing a calmodulin (CaM) binding site as well as other regulatory domains. Originally discovered in erythrocyte membranes (Schatzmann, 1966), PMCAs were subsequently shown to be ubiquitous mechanisms for high-affinity Ca^{2+} extrusion across membranes of eukaryotic cells. Primary structure was first cloned in rat and human (Shull and Greeb, 1988; Verma et al., 1988). Early progress was hampered by the low abundance of these proteins but, to date, there is a comprehensive literature on enzymatic properties, biochemical regulation, gross functional domain structure and primary amino acid sequences, although largely restricted to vertebrate species (Carafoli, 1991, 1994; Carafoli and Stauffer, 1994; Monteith and Roufogalis, 1995; Lehotsky, 1995; Penniston and Enyedi, 1998; Guerini et al., 1999, 2000). In vertebrates, research has focused primarily on excitable tissues, although some studies have involved intestinal absorptive epithelia (Borke et al., 1990; Howard et al., 1994) and mammary secretory epithelium (Reinhardt and Horst, 1999).

Mammalian PMCAs are encoded by four non-allelic genes located on different chromosomes, and additional isoform variants (as many as 30 in total) are generated *via* alternative RNA splicing of the primary gene transcripts at two major regulatory sites, one adjacent to the amino-terminal phospholipid responsive region and another within the carboxyl-terminal CaM binding domain (Olson et al., 1991; Brandt et al., 1992; Latif et al., 1993; Wang et al., 1994). The four *PMCA* genes appear to be very closely related in their exon–intron structure (Burk and Shull, 1992; Hilfiker et al., 1993; Kuzmin et al., 1994). General consensus in vertebrates is that *PMCAs* 1 and 4 are found in virtually all tissues and appear to be ‘housekeeping’ isoforms whereas *PMCA* 2 and 3 are subject to temporal and spatial tissue- and cell-specific regulation and, as such, may inform the functional adaptation to the physiological need of preserving multiple isoforms over many years of evolution (Burk and Shull, 1992; Carafoli and Stauffer, 1994). The substantial differences among *PMCA* isoforms are in their regulation by kinases, proteases and the Ca^{2+}-binding protein CaM (Borke et at., 1990; Carafoli, 1991; Axelsen and Palmgren, 1998; Bourinet et al., 1999).

PMCA3 was the isoform selected for complete characterization based on preliminary studies in our lab and the fact that it has emerged from mammalian studies as a candidate isoform for tissue-specific and developmental regulation and alternative splicing patterns. The freshwater crayfish molting cycle can offer unique insights into the spatial and temporal regulation of PMCAs during unidirectional Ca^{2+} influx. In the present study, we set out to clone and characterize PMCA3 in crayfish tissues and to compare tissue-specific expression as a function of the molting cycle in both Ca^{2+}-transporting epithelia (gill/antennal gland) and non-Ca^{2+}-transporting tissues (axial and cardiac muscle). We hypothesized that PMCA3 would be upregulated in Ca^{2+}-transporting epithelia in pre- and postmolt compared with intermolt and that levels in non-transporting epithelia would be unchanged.

Materials and methods

Animal material

Crayfish, *Procambarus clarkii* (Girard), were obtained from Carolina Biological Supply (Burlington, NC, USA) and maintained in 40-liter aquaria in filtered aerated water at room temperature (RT; 23°C). Tissues were removed from animals at various stages in the natural molting cycle. Premolt status was determined from the gastrolith index (McWhinnie, 1962). Postmolt status was classified in reference to the day of ecdysis (shedding). Following decerebration, the cardiac muscle, axial abdominal muscle, antennal gland (kidney) and gill were dissected out.

Isolation of total RNA and mRNA

After dissection, tissues were frozen immediately in liquid nitrogen and stored at –80°C. Total RNA was isolated by utilizing Trizol reagent (Invitrogen, Carlsbad, CA, USA), as specified by the manufacturer. Briefly, 0.5 g of tissue was finely ground in liquid N_2 and lysed by adding 3 ml of Trizol reagent. The lysates were allowed to incubate at RT for 5 min. Then, 1.2 ml chloroform was added followed by vigorous vortexing for 15 s. Samples were then incubated for 5 min at RT and centrifuged for 15 min at 13 362 ***g***. Following removal of the aqueous phase and addition of 1.5 ml of isopropanol, samples were placed at –80°C overnight and then centrifuged for 15 min at 13 362 ***g***. The RNA pellets were washed with 1.5 ml 75% ethanol, sedimented for 5 min at 7516 ***g*** and air-dried for 10 min before being dissolved in diethyl pyrocarbonate (DEPC)-treated water and stored at –80°C. Messenger RNA was separated from total RNA using an oligo-dT cellulose column (Stratagene, La Jolla, CA, USA). RNA or mRNA was quantified spectrophotometrically at wavelengths of 260 and 280 nm.

Cloning of crayfish antennal gland (kidney) PMCA3

We elected to clone the *PMCA3* initially from antennal gland because physiological studies had indicated that it exhibited higher rates of intermolt unidirectional Ca^{2+} influx than any other epithelial tissue (Wheatly, 1999). First-strand cDNA was reverse transcribed from 400 ng of mRNA from antennal gland using the SuperScript II RNase H-reverse transcriptase (Gibco BRL, Gaithersburg, MD, USA) with oligo$(dT)_{12–18}$ as primer. Based on four published *PMCA3* sequences from human (GenBank accession nos US57971 and U60414; Brown et al., 1996), mouse (AKO32322; Carninci et al., 2000) and rat (J05087; Greeb and Shull, 1989), two primers were designed: 5′-GGGCAAYGCCACAGCCATCT-3′ (sense) and 5′-CCCCACATGACYGCCTTGACR-3′ (antisense). Primer location corresponded to nucleotides 1518–2652 in human, 1686–2820 in mouse and 2045–3179 in rat. These primers targeted a fragment of approximately 1134 bp located between transmembrane regions TM4 and TM5 of the *PMCA3* gene in human, mouse and rat. Polymerase chain reactions (PCR; total volume 50 μl) included 2 μl of first-strand cDNA from postmolt antennal gland, 20 mmol l^{-1} Tris HCl (pH 8.4), 50 mmol l^{-1} KCl, 1.5 mmol l^{-1} $MgCl_2$, 0.2 mmol l^{-1} dNTP mix, 0.1–0.2 μmol l^{-1} of each primer and 2.5 units of Taq DNA polymerase (Gibco BRL). RT-PCR cycles were conducted at 94°C for 3 min followed by 30 cycles of 94°C for 30 s, 58.5°C for 1 min, 72°C for 1 min and a final extension at 72°C for 10 min. Negative controls in which reactions contained no template cDNA were included. RT-PCR products were analyzed by electrophoresis on a 1.0% agarose gel with 0.5 μg ml^{-1} of ethidium bromide in 1× TAE buffer (40 mmol l^{-1} Tris, 40 mmol l^{-1} sodium acetate and 1 mmol l^{-1} EDTA, pH 7.2). The DNA bands were visualized with ultraviolet light.

Subsequently, 3′ and 5′ RACE (rapid amplification of cDNA ends) systems (Invitrogen) were used to amplify the 3′ and 5′ ends of crayfish antennal gland *PMCA3*. For the 5′ RACE, a gene-specific primer, 5′-GAGGGTGCCAGTCTTGTCA-3′, and a nested primer, 5′-AGGCATCCAGGTGGCGCACCA-3′, were used. For the 3′ RACE, a gene-specific primer, 5′-AGGCCTCAGACATCATTCTGAC-3′, and a nested primer, 5′-TGTCAAGGCTGTCATGTGGGG-3′, were designed. The PCR conditions were the same as described above. The integrity of the RNA from the various tissues was checked by the presence of a fragment of 18s ribosomal RNA gene. The RNA 18s primers (sense 5′-GGCCCAGACACCGGAAGG-ATTGAC-3′ and antisense 5′-GCCCGAGACGCGAGGGGT-AGAACA-3′) were designed from *Procambarus clarkii.*

18s ribosomal RNA gene, coding for a 518 bp fragment (accession no. AF436001)

PCR products were ligated to PCR 2.1 vector (Invitrogen) for transformation into INVF host cells (Invitrogen). Each clone was digested with appropriate restriction enzymes and subcloned for sequencing. Two independent clones were sequenced from both ends. The cDNA clones were sequenced by automated sequencing (ABI PRISM 377, 3100 and 3700 DNA sequencers; Davis Sequencing, Foster City, CA, USA).

The complete sequence was assembled with DNASTAR (DNASTAR Inc., Madison, WI, USA). Sequence homology was revealed through a GenBank database search using the BLAST algorithm search (http://www.ncbi.nlm.nih.gov/blast).

Northern blot

Northern blot analysis was performed to determine the distribution of *PMCA3* in gill, antennal gland, cardiac muscle and axial abdominal muscle during various stages of the molting cycle. Total RNA (25 μg) from each tissue examined was fractionated by electrophoresis through a 0.72 mol l^{-1} formaldehyde–1% agarose denaturing gel, run in MOPS buffer (5 mmol l^{-1} sodium acetate, 1 mmol l^{-1} EDTA, 20 mmol l^{-1} MOPS at pH 6.6) and transferred overnight to a Nytran Plus membrane (Schleicher & Schuell, Keene, NH, USA) by capillary elution in 10× SSC (where 1× SSC is 150 mmol 1^{-1} NaCl, 15 mmol 1^{-1} sodium citrate). RNA was fixed by ultraviolet crosslinking using a UVC-515 ultraviolet multilinker from Ultra-Lum (Claremont, CA, USA; 120 000 μJ cm^{-2}). An RNA molecular mass marker (a 0.24–9.5 kb ladder) was run along with the samples, then visualized with ultraviolet light after staining with ethidium bromide, and used for the standard curve. The membrane was prehybridized for 4 h at 68°C in 6× SSC, 2× Denhardt's reagent (0.4 g Ficoll type 400, 0.4 g polyvinylpyrrolidone, 0.4 g bovine serum albumin in 1 liter water), 0.1% SDS and 100 ng ml^{-1} denatured salmon sperm DNA. Hybridization was performed overnight at 68°C in the prehybridization solution with 20 ng of *PMCA* antennal gland isoform cDNA probe that was randomly labeled with [α-^{32}P]dATP. The membrane was washed four times for 15 min at 60°C in 0.1× SSC and 0.1% SDS. The membrane was exposed to X-ray film with intensifying screens at –80°C. To normalize the hybridization signal, 18s RNA was quantified on a corresponding formaldehyde–agarose gel. Total RNA content was determined by OD_{260} and visualized by ethidium bromide staining.

Western blot

Membrane protein from gill, antennal gland, cardiac muscle and axial abdominal muscle was prepared from freshly isolated tissue using differential centrifugation following published methodology (Williams et al., 1999). Briefly, 0.5 g tissue was dissected and ground first in liquid N_2 and then in 1 ml of homogenization buffer (250 mmol l^{-1} sucrose, 10 mmol l^{-1} Tris, 10 mmol l^{-1} Hepes, 1 mmol l^{-1} EDTA; pH adjusted to 7.2 at 23°C) containing protease inhibitors for an additional 3–5 min. Following centrifugation at 4547 ***g*** for 10 min at 4°C, the supernatant was centrifuged at 6100 ***g*** for 30 min at 4°C. The final pellet was resuspended in ~100–500 µl of homogenization buffer with protease inhibitors and stored at –80°C. Protein concentration was determined using a Micro-BCA protein kit (Pierce, Rockford, IL, USA).

Membrane proteins were separated by 9% SDS–polyacrylamide gel electrophoresis and transferred from unstained gels to nitrocellulose membranes (Bio-Rad, Hercules, CA, USA) in transfer buffer (192 mmol l^{-1} glycine, 25 mmol l^{-1} Tris-HCl, pH 8.3) overnight at 30 V using a Bio-Rad Trans-Blot tank apparatus. Nitrocellulose-bound protein was visualized by staining with Coomassie Brilliant Blue R-250. The nitrocellulose membrane was blocked overnight in PBS/milk (7% nonfat dry milk and 0.1% Tween 20 in PBS, pH 7.4) at 23°C and then incubated in PBS/milk with 1:1000 purified anti-PMCA3 polyclonal antibody for 2 h at 23°C. After three 10 min washes in PBS/milk, the nitrocellulose membrane was incubated with secondary antibody at 1:2000 dilution (horseradish peroxidase conjugated goat anti-rabbit IgG) for 1 h at 23°C in PBS/milk. After three washes in PBS, 0.1% Tween 20, bound antibody was detected using ECL western blotting detection reagents (Amersham Pharmacia Biotech, Piscataway, NJ, USA).

To generate the PMCA3 antibody, an amino acid sequence deduced from crayfish *PMCA3* cDNA sequence was used to design an antigenic oligo-peptide (Boersma et al., 1993). The designed oligo-peptide – EGKEFNRRVRDESGC from amino acid residues 751–775 located in the cytosolic loop before the FSBA {γ-[4-(*N*-2-chloroethyl-*N*-methylamino)] benzylamine ATP binding} site – was synthesized commercially (Genemed Biotech Inc., San Francisco, CA, USA). To increase antigenicity, the oligo-peptide was conjugated to cBSA (cationized BSA; Pierce). The antigenic peptide was subsequently used for production of a polyclonal antibody in New Zealand White rabbits in compliance with LACUC protocol AUP 245 issued to Dr Harold Stills, WSU Veterinarian. Trained LAR staff performed all the injections and blood collections following the euthanasia procedures. Antiserum titer was determined by enzyme-linked immunosorbent assays (ELISAs) using synthetic peptide as antigen (Wheatly et al., 2001).

Northern and western blots were repeated in triplicate and quantified through scanning the X-ray film images using KODAK 1D image analysis software (Scientific Imaging System, Eastman Kodak Company, Rochester, NY, USA).

Results

Cloning of crayfish antennal gland PMCA3

The primers 5′-GGGCAACGCCACAGCCATCT-3′ (sense) and 5′-CCCCACATGACCGCCTTGACA-3′ (antisense), designed based on three published *PMCA3* sequences from human, mouse and rat, were successful in amplification of a discrete product from crayfish antennal gland. The size of the PCR product was 1164 bp, containing 30 more nucleotides (567–597 bp) than expected. A search of the GenBank database using the BLAST algorithm (Altschul et al., 1990) confirmed that the nucleotide sequence matched exclusively with *PMCA3* from human, mouse and rat with 78–80% identity. This partial sequence provided crucial DNA sequence information required for 5′ and 3′ RACE cloning of the complete *PMCA3* sequence. Using 3′ RACE, a 1496 bp fragment with a poly(A) tail at the 3′ end was obtained. A BLAST search of this fragment matched at the level of 83–85% with human, rat and mouse *PMCA3*. By using the 5′ RACE technique, a 1478 bp fragment was amplified. The BLAST search indicated that this fragment had 77–79% similarity with human, mouse and rat *PMCA3*.

Overall, the complete crayfish antennal gland *PMCA3* nucleotide sequence contains 4148 nucleotides with an open reading frame of 3546 bp coding for 1182 amino acid residues with a molecular mass of 130 kDa (Fig. 1A). There is a 559 bp noncoding sequence at the 3′ end before the poly(A) region and a 40 bp noncoding sequence at the 5′ end. A search of the GenBank database using the BLAST algorithm indicated that this crayfish *PMCA3* sequence is homologous with over 55 *PMCAs*, including *PMCA3*, *PMCA2*, *PMCA1* and *PMCA4*, and shares the highest homology (77.5–80.9% identity at the DNA level) with human brain *PMCA3* isoforms a and b (GenBank accession nos U57971 and U60414; Brown et al., 1996), rat *PMCA3* (J05087; Greeb and Shull, 1989), mouse retinal neuron *PMCA3b* (NM177236; Krizaj et al., 2002) and mouse brain *PMCA3* (AKO32322; Carninci et al., 2000). The deduced amino acid sequence also shares high homology (85.3–86.9%) with PMCA3 from human, mouse and rat. Therefore, this sequence was confirmed as crayfish antennal gland *PMCA3*. A BLAST search indicated that the crayfish *PMCA3* also shared relatively high homology with *PMCA2* sequences including mammalian *PMCA2* and *PMCA2* from non-mammalian species, such as bullfrog *PMCA2a* (AF337956; R. A. Dumont, U. Lins, A. G. Filoteo, J. Penniston, B. Kachar and P. G. Gillespie, direct submission to GenBank in 2001, no accompanying publication) and tilapia *PMCA2* (AF236669; C.-H. Yang, J.-H. Leu, C.-M. Chou, S.-P. L. Hwang, C.-J. Huang and P. P. Hwang, direct submission to GenBank in 2000, no accompanying publication). Fig. 1B shows the alignment of crayfish PMCA3 deduced amino acid sequence with human PMCA3a. Because PMCA3 sequences were not available from non-mammalian species, two PMCA2 sequences (from tilapia and bullfrog) were also included in Fig. 1.

Comparing the crayfish PMCA3 amino acid sequence to other PMCAs, the first intracellular loop region between TM2 and TM3 is one region where major sequence differences occur (Fig. 1B). This region corresponds to the 'transduction domain', thought to play an important role in the long-range transmission of conformational changes occurring during the transport cycle. The other major differences occur in the C-terminus immediately 3′ to the CaM binding site. This region is believed to be the location of regulation by kinases, proteases and CaM. Amino acid sequences at this region after IQTQ of the CaM binding site vary from 40 to 107 residues in length, and the identity at this region drops to less than 67%. Furthermore, as mentioned before, crayfish PMCA3 has a 10-amino-acid insertion not found in other PMCA3 and PMCA2 sequences at the region between the FITC (fluorescein isothiocyanate) and the FSBA site.

Comparison among sequences indicates that some regions have virtually 100% identity (TM1, TM2, TM4, phosphorylation site, FITC site, FSBA site, TM5, TM6, TM8 and CaM binding site). Other regions exhibit less identity (TM7 and TM10). Interestingly, there were some regions where crayfish antennal gland PMCA3 exhibited a closer identity to mammalian PMCA3 sequences than to fish or amphibian PMCA2 sequences (TM3 and TM9).

The hydropathy profile of crayfish PMCA3 was compared with those sequences from other species named above (Fig. 2). The predicted amino acid sequence of crayfish PMCA3 displays a structure common to other PMCA pumps. It appears that the crayfish PMCA3 contains 10 membrane-spanning segments, as indicated in other PMCAs. Four of these putative transmembrane domains are located near the N-terminal region and the remaining six are located near the C-terminus, with a large cytoplasmic loop in between. The bulk of the protein mass is facing the cytosol and consists of three major domains: the IC loop between TM 2 and TM3, the large unit between TM4 and TM5, and the extended 'tail' following the last transmembrane domain. The large cytosolic region (~400 residues) of crayfish antennal gland PMCA3 between membrane-spanning segments 4 and 5 contains the major catalytic domains, including the ATP binding site and the invariate aspartate residue that forms the acylphosphate intermediate during ATP hydrolysis.

Crayfish PMCA3 *mRNA expression during the molting cycle*

The tissue distribution of this novel crayfish *PMCA3* gene was examined using a northern blot of total RNA from crayfish gill, antennal gland, cardiac muscle and axial abdominal muscle tissues probed with the 1164 bp fragment initially cloned that corresponded to nucleotides 1488–2652. In all four tissues examined, the probe detected a 7.5 kb mRNA (Fig. 3). The expression of *PMCA3* mRNA in all four tissues increased during both premolt and postmolt compared with intermolt (Fig. 3); when these changes were quantified (Fig. 4A), the increases observed in *PMCA3* mRNA expression in the Ca^{2+}-transporting epithelia (gill and antennal gland) were about double (60% increase) the increases in non-Ca^{2+}-transporting tissues (about 25% increase in cardiac and axial muscle). The only tissue that exhibited a significant further increase in mRNA expression in postmolt as compared with premolt was the antennal gland.

Crayfish PMCA3 protein expression during the molting cycle

PMCA3 protein expression was confirmed through western blotting. A polyclonal antibody against crayfish PMCA3 recognized a 130 kDa protein band that was just detectable in all tissues in the intermolt stage (Fig. 5). Protein expression increased markedly during pre- and postmolt stages as compared with intermolt in all four tissues (Fig. 5), generally confirming the trend observed in mRNA expression. Quantification of protein expression (Fig. 4B) in gill and antennal gland paralleled the trends observed above in mRNA expression (Fig. 4A), namely that expression in antennal gland increased further in postmolt compared with premolt while expression in gill was unchanged. A second isoform band (128 kDa) was apparent primarily in axial muscle, where it appeared to be the prominent band in intermolt. Expression of this band did not seem to change during the molting cycle (Fig. 5). Unexpectedly, PMCA3 protein expression in muscle increased significantly in postmolt compared with premolt, unlike mRNA expression, which remained unchanged.

Discussion

Preliminary work revealed that there are four *PMCA* genes in crayfish (Y.G. and M.G.W., unpublished), as there are in vertebrates, suggesting that selective pressure has maintained four isoforms throughout evolution because each plays a unique and critical role in cell function (Lutsenko and Kaplan, 1995). Studying these genes and their expression patterns in invertebrates will inform the molecular evolution of these important proteins in mammals. Preliminary RT-PCR indicated that there is one species of *PMCA1* that appeared to be a 'housekeeping' isoform. *PMCA1* was the first gene to be expressed during mouse embryo development (Zacharias and Kappen, 1999); the other three isoforms were not detectable until day 12.5, and all showed pronounced changes in the level and/or tissue distribution during further development.

Preliminary studies (Y.G. and M.G.W., unpublished) indicated that there are at least two species of all other isoforms. Seemingly, there are several splice variants in crayfish, suggesting that alternative splicing generates significant isoform diversity as it does in mammals (Shull and Greeb, 1988; Strehler, 1991; Burk and Shull, 1992; Stauffer et al., 1993; Zacharias et al., 1995; Keeton and Shull, 1995). Alternative splicing affects two major locations in the PMCA protein that correspond to the major regulatory domains: firstly, a region embedded between a putative G protein binding sequence and the site of phospholipid sensitivity in the first cytosolic loop; and secondly a region in the COOH-terminal tail that affects regulation by CaM, phosphorylation

```
A atgggcgacgatgccaatagttcaatcgagttccaccccaggcccaaccagcgccgggat   60
   M  G  D  D  A  N  S  S  I  E  F  H  P  R  P  N  Q  R  R  D    20
  ggcaaccaggctggcggctttgggtgctcactgatggagctgcgcagcctcatggagctg  120
   G  N  Q  A  G  G  F  G  C  S  L  M  E  L  R  S  L  M  E  L    40
  cgagggcttgaggcggtggttaagatccaggaggactacggggatgtcgaagggctctgc  180
   R  G  L  E  A  V  V  K  I  Q  E  D  Y  G  D  V  E  G  L  C    60
  aggaggctgaagacctcacccacagagggtctggcggacaacaccaatgacctggagaag  240
   R  R  L  K  T  S  P  T  E  G  L  A  D  N  T  N  D  L  E  K    80
  cgcaggcagatctacgggcagaacttcatcccgccaaagaaacccaaaaccttcctgcag  300
   R  R  Q  I  Y  G  Q  N  F  I  P  P  K  K  P  K  T  F  L  Q   100
  ctggtgtgggaggcgctgcaggacgtgactctcatcatcctggaaatagcggccattgtg  360
   L  V  W  E  A  L  Q  D  V  T  L  I  I  L  E  I  A  A  I  V   120
  tccctgggtctgtcgttctatagaccgccaggagaaaccggaggtggagcggcggcaggt  420
   S  L  G  L  S  F  Y  R  P  P  G  E  T  G  G  G  A  A  A  G   140
  ggggccgaagatgagggtgaagcagaagctggttggattgagggtgctgcaatcctttta  480
   G  A  E  D  E  G  E  A  E  A  G  W  I  E  G  A  A  I  L  L   160
  tctgtagtgtgtgtggtgctggtcacggccttcaatgactggagcaaggagaagcagttc  540
   S  V  V  C  V  V  L  V  T  A  F  N  D  W  S  K  E  K  Q  F   180
  cgaggcctacagagccgtattgaacaggagcagaaatttactgtggtccgtaacggacag  600
   R  G  L  Q  S  R  I  E  Q  E  Q  K  F  T  V  V  R  N  G  Q   200
  gtccttcagatccccgtggctgaacttgtggtcggggacattgcccaggtcaagtatggt  660
   V  L  Q  I  P  V  A  E  L  V  V  G  D  I  A  Q  V  K  Y  G   220
  gacctgctaccagcggatggtgtgttgatacagggaaatgacctgaagatagacgagagg  720
   D  L  L  P  A  D  G  V  L  I  Q  G  N  D  L  K  I  D  E  R   240
  tccttaacgggagagtctgaccatgtccgcaaatcggctgacaaagatccaatgctgctc  780
   S  L  T  G  E  S  D  H  V  R  K  S  A  D  K  D  P  M  L  L   260
  tcagggactcatgtgatggaagggtccggaagaatggtggtcactgccgttggggtgaat  840
   S  G  T  H  V  M  E  G  S  G  R  M  V  V  T  A  V  G  V  N   280
  tctcagactggaatcatcttcacgctgctcggagctggagcggaggaagaagaggttgaa  900
   S  Q  T  G  I  I  F  T  L  L  G  A  G  A  E  E  E  E  V  E   300
  gcgaagaaacgaaaaaaagaggccaaaaagcagcggaaaaaacagaaaaagggcgactcg  960
   A  K  K  R  K  K  E  A  K  K  Q  R  K  K  Q  K  K  G  D  S   320
  ggcgaagagttgattgacgccaatcctaagaagcaggatggggagatggagagcaaccag 1020
   G  E  E  L  I  D  A  N  P  K  K  Q  D  G  E  M  E  S  N  Q   340
  atcaaagctaaaaaacaggatggagcagctgccatggagatgcagcccctgaagagtgct 1080
   I  K  A  K  K  Q  D  G  A  A  A  M  E  M  Q  P  L  K  S  A   360
  gaaggtggagaggctgacgaggaagaggagaagaaagtcaacacaccgaagaaagagaag 1140
   E  G  G  E  A  D  E  E  E  E  K  K  V  N  T  P  K  K  E  K   380
  tctgtgctgcaggggaagctgaccaagctggctgtgcagattgggaaagcaggtttggtg 1200
   S  V  L  Q  G  K  L  T  K  L  A  V  Q  I  G  K  A  G  L  V   400
  atgtctgccatcacagtcatcatcctggtactctactttggtattgaaacttttgttgtg 1260
   M  S  A  I  T  V  I  I  L  V  L  Y  F  G  I  E  T  F  V  V   420
  gaagggagaccctggactccagtttatatccaatatttgtcaagttcttcatcattggt 1320
   E  G  R  P  W  T  P  V  Y  I  Q  Y  F  V  K  F  F  I  I  G   440
  gtcactgtgctggtggtggctgtcccggagggcctcccactggctgtcaccatatcacta 1380
   V  T  V  L  V  V  A  V  P  E  G  L  P  L  A  V  T  I  S  L   460
  gcttactctgtcaagaaaatgatgaaagacaacaacttggtgcgccacctggatgcctgt 1440

   A  Y  S  V  K  K  M  M  K  D  N  N  L  V  R  H  L  D  A  C   480
                                  Nested primer for 5'RACE
  gagaccatgggcaacgccacagccatctgctctgacaagactggcaccctcacaaccaac 1500
   E  T  M  G  N  A  T  A  I  C  S  D  K  T  G  T  L  T  T  N   500
                                      Phosphorylation
       Initial PCR sense primer
                           Gene specific primer for 5'RACE
  cgtatgactgtggttcagtcgtacataggtgatgagcactacaaagagataccagaccct 1560
   R  M  T  V  V  Q  S  Y  I  G  D  E  H  Y  K  E  I  P  D  P   520
  ggatccctaccacctaagattctagatcttctggtcaatgccatttcaatcaacagtgcc 1620
   G  S  L  P  P  K  I  L  D  L  L  V  N  A  I  S  I  N  S  A   540
  tatacaaccaaaatactgccaccagacaaggaaggagatctcccacggcaggtgggcaat 1680
   Y  T  T  K  I  L  P  P  D  K  E  G  D  L  P  R  Q  V  G  N   560
  aagaccgagtgcgctttgctaggatttgtcttggaccttaagcgggactatcagcccatc 1740
   K  T  E  C  A  L  L  G  F  V  L  D  L  K  R  D  Y  Q  P  I   580
  cgtgatcaaatccctgaagaaaagctgtacaaagtgtacacctttaactctgtcagaaaa 1800
   R  D  Q  I  P  E  E  K  L  Y  K  V  Y  T  F  N  S  V  R  K   600
                                                    FITC
  tccatgagcacggtcgtgcctatgcgagacggaggtttccgcatctacagcaaaggggcc 1860
   S  M  S  T  V  V  P  M  R  D  G  G  F  R  I  Y  S  K  G  A   620
  tcagagatcgtcttgaaaaagtgctcccagatcctgaacagggatggcgaactaaggagc 1920
   S  E  I  V  L  K  K  C  S  Q  I  L  N  R  D  G  E  L  R  S   640
  ttccggccgcgggataaagatgatatggttagaaaagtcattgaacccatggcgtgtgat 1980
   F  R  P  R  D  K  D  D  M  V  R  K  V  I  E  P  M  A  C  D   660
  ggactccgcacaatctgcattgcataccgggactttgttcgaggatgcgctgaaataaac 2040
   G  L  R  T  I  C  I  A  Y  R  D  F  V  R  G  C  A  E  I  N   680
  caggtccactttgaaaatgaacccaactgggacaacgaaaataacattatgagcgacctg 2100
   Q  V  H  F  E  N  E  P  N  W  D  N  E  N  N  I  M  S  D  L   700
  acttgcctagctgttgtgggcattgaagatccagtgcggcccgaggtacctgatgccatc 2160
   T  C  L  A  V  V  G  I  E  D  P  V  R  P  E  V  P  D  A  I   720
  caaaaatgccagcgggctggcattacagttcgcatggtaaccggcgcaaatatcaacact 2220
   Q  K  C  Q  R  A  G  I  T  V  R  M  V  T  G  A  N  I  N  T   740
  gcacgcgccattgcttccaaatgtggcatcatccaaccaggagaggatttcctttgcttg 2280
   A  R  A  I  A  S  K  C  G  I  I  Q  P  G  E  D  F  L  C  L   760
  gaaggaaaagagtttaacaggaggattagagatgagtcgggctgcatcgaacaagagaga 2340
   E  G  K  E  F  N  R  R  I  R  D  E  S  G  C  I  E  Q  E  R   780
        Crayfish PMCA3 Ab peptide
  atagacaaggtgtggccgaagctgcgtgtgctggcccgctcatctcctacagacaaacac 2400
   I  D  K  V  W  P  K  L  R  V  L  A  R  S  S  P  T  D  K  H   800
  acactggtgaaaggtattatagacagcacaacaaatgaccaaaggcaagtggtggctgta 2460
   T  L  V  K  G  I  I  D  S  T  T  N  D  Q  R  Q  V  V  A  V   820
  actggtgatgggaccaacgatggccctgccctcaaaaaggctgatgtcggctttgccatg 2520
   T  G  D  G  T  N  D  G  P  A  L  K  K  A  D  V  G  F  A  M   840
            FSBA-Site
  ggcatcgctggtactgatgttgcaaaggaggcctcagacatcattctgacagatgacaac 2580
   G  I  A  G  T  D  V  A  K  E  A  S  D  I  I  L  T  D  D  N   860
                      Gene specific primer for 3'RACE
  Ttcaccagcattgtcaaggctgtcatgtgggggcgcaatgtatatgacagcatttccaaa 2640
   F  T  S  I  V  K  A  V  M  W  G  R  N  V  Y  D  S  I  S  K   880
            Initial PCR antisense primer
           Nested primer for 3'RACE
  ttcctacaatttcagctgacagtcaatgtcgtggctgttatcgtagcatttacaggtgcc 2700
   F  L  Q  F  Q  L  T  V  N  V  V  A  V  I  V  A  F  T  G  A   900
  tgcatcactcaggactctcctcttaaggctgtgcagatgttgtgggtgaaccttatcatg 2760
   C  I  T  Q  D  S  P  L  K  A  V  Q  M  L  W  V  N  L  I  M   920
  gacacattcgcttccctggcattggcgacggaaccaccaacggagtctctcctgctgcga 2820
   D  T  F  A  S  L  A  L  A  T  E  P  P  T  E  S  L  L  L  R   940
  aaaccctatggtcgcaccaaacctctcatctcgcgcaccatgatgaagaatattctgggt 2880
   K  P  Y  G  R  T  K  P  L  I  S  R  T  M  M  K  N  I  L  G   960
  cacgccgtgtaccagcttctaattatattcactttgctatttgttggtgagggcttcttc 2940
   H  A  V  Y  Q  L  L  I  I  F  T  L  L  F  V  G  E  G  F  F   980
  gacatcgacagtggaaggaatgctcccctgcactctccaccttccgagcactacaccatc 3000
   D  I  D  S  G  R  N  A  P  L  H  S  P  P  S  E  H  Y  T  I  1000
  atcttcaacactttcgttatgatgcagctcttcaatgagatcaacgcccgcaagatccac 3060
   I  F  N  T  F  V  M  M  Q  L  F  N  E  I  N  A  R  K  I  H  1020
  ggcgaaaggaacgtcttcgacggcatcttcagcaaccccatcttctgcacgattgtccta 3120
   G  E  R  N  V  F  D  G  I  F  S  N  P  I  F  C  T  I  V  L  1040
  ggcaccttcggaatccaaattgtcatcgtccagtttggcgggaagccctttagctgcacc 3180
   G  T  F  G  I  Q  I  V  I  V  Q  F  G  G  K  P  F  S  C  T  1060
  ccgctgcccgcggaacagtggctctggtgtctttttgttggtgctggggaactggtctgg 3240
   P  L  P  A  E  Q  W  L  W  C  L  F  V  G  A  G  E  L  V  W  1080
  gggcaggtcatggccaccatccccaccagccagcttaagtcgctgaagggggccgggcac 3300
   G  Q  V  M  A  T  I  P  T  S  Q  L  K  S  L  K  G  A  G  H  1100
  gagcacaggaaagacgaaatgaatgctgaggacctgaacgaaggccaggaagagatcgac 3360
   E  H  R  K  D  E  M  N  A  E  D  L  N  E  G  Q  E  E  I  D  1120
  catgccgagagggagctccgcagaggtcagatcctctggttccggggcctcaaccggatc 3420
   H  A  E  R  E  L  R  R  G  Q  I  L  W  F  R  G  L  N  R  I  1140
                       CaM biding site
  cagacacagattgaagtagtgaatgccttcaagagtggcagttctgttcaggggggctgtg 3480
   Q  T  Q  I  E  V  V  N  A  F  K  S  G  S  S  V  Q  G  A  V  1160
  cggcgaccatcctccatcctcagccagaaccaagatgtaacaaatgtttctacccctagt 3540
   R  R  P  S  S  I  L  S  Q  N  Q  D  V  T  N  V  S  T  P  S  1180
  cacggctag                                                    3549
   H  G  .                                                     1183
```

Fig. 1. (A) Nucleotide sequence of open reading frame (ORF) and deduced amino acid sequence of crayfish antennal gland plasma membrane Ca^{2+}-ATPase (PMCA3). Nucleotides and amino acids are numbered on the right. The putative start codon ATG and stop codon TAG are in bold. Sequences corresponding to the primers used in both initial PCR and 5′/3′ RACE are underlined. (B) Comparison of the deduced amino acid sequence of crayfish antennal gland plasma membrane Ca^{2+}-ATPase (PMCA3) with that of human PMCA3a (GenBank accession No. U57931), tilapia PMCA2 (AF23669) and bullfrog PMCA2a (AF337956). Stars below amino acids indicate identity between residues in PMCA from different species. Amino acids are numbered on the right. Transmembrane regions are underlined and labeled TM1–TM10. The phosphorylation site, fluorescein isothiocyanate (FITC) site (assumed to be part of the ATP-binding site), the 5′-*p*-fluorosulphonylbenzoyladenosine/r-(*N*-2-chloroethyl-*N*-methylamino) benzylamine ATP-binding (FSBA) site, calmodulin (CaM) binding site and PMCA3 Ab peptides location are underlined in both A and B. This sequence has been accepted by GenBank (accession number AY455931).

and differential interaction with PDZ domain-containing anchoring and signaling proteins (De Jaegere et al., 1990; Strehler et al., 1990; Strehler, 1991).

The present paper describes the cloning of *PMCA3* from the antennal gland of crayfish *Procambarus clarkii* as well as the regulation of both mRNA and protein tissue-specific expression during the natural molting cycle. This is the first *complete* sequence from an invertebrate with the exception of several isoforms cloned as part of the *Caenorhabditis elegans* genome project [Kraev et al., 1999 initially cloned mca-1 (GenBank accession no. NM_069308) and mca-2 (NM_067760); later, Kamath et al. (2003) identified mca-3 (NM_067893) with ‘a’ (AAK685500); ‘b’ (AAK68551) and ‘c’ (AAM97979) splice variants (Waterston, 1998)]. A partial sequence is available for the isopod *Porcellio scaber* (AF455814; Ziegler et al., 2002). Aside from one *PMCA2* sequence from a fish (*Oreochromis mossambicus*, tilapia; AF23669; C.-H. Yang, J.-H. Leu, C.-M. Chou, S.-P. L.

B

```
Crayfish 3  MGDMANSSIEFHPKPNQRRDGNQAGGFGCSLMELRSLMELRGVEAVVKLQ    50
Human 3a    ***************Q*Q**VP*******T*A**********A*****IE    50
Tilapia 2   *******–-D*YA*-***NE**H*AA***************T*******    47
Bullfrog 2a ****S**--D*YS*-***NEV*H*SE***T*D**********T*****I*    47

Crayfish 3  EDYGDVEGLCRRLKTSPTEGLADNTNDLEKRRQIYGQNFIPPKKPKTFLQ   100
Human 3a    *A**D*S**************D********************Q******   100
Tilapia 2   ****G*E**************GAQT**D**K******L***********    97
Bullfrog 2a *****TD*************PGTQA*******V****************    97

Crayfish 3  LVWEALQDVTLIILEIAAIVSLGLSFYRPPGETG-G--GAAAGGAHDEGE   147
Human 3a    ***************V***********A****ES-*A**NVS********   149
Tilapia 2   ******************LI*******H****T**ESC************   147
Bullfrog 2a *******************I*************TE*CG*******E****   147
                   TM1

Crayfish 3  AEAGWIEGAAILISVVCVVLVTAFNDWSKEKQFRGLQSRIEQEQKFTVVR   197
Human 3a    ***************I*********************************I*   199
Tilapia 2   *D*****************************************Q***   197
Bullfrog 2a *D************************************************   197
                        TM2

Crayfish 3  NGQVLQIPVAELVVGDIAQVKYGDLLPADGVLIQGNDLKIDESSLTGESD   247
Human 3a    ***L**V***A**********************A****************   249
Tilapia 2   ****I*L****I*******I*******S**********************   247
Bullfrog 2a *S**I*******V*************************************   247

Crayfish 3  HVRKSADKDPMLLSGTHVMEGSGRMVVTAVGVNSQTGIIFTLLGAGAEEE   297
Human 3a    **********************************************G***   299
Tilapia 2   **********************************************V***   297
Bullfrog 2a ****AV*****************L*******************SEM*D*   297

Crayfish 3  EVEAKKRKK------------EAKKQRKKQKKGDSGEELIDA------NP   329
Human 3a    *--------------------------**D***----------------   306
Tilapia 2   *KKE**GGAVEDG-----------------------------------HQNTG   315
Bullfrog 2a *KKD**G**NQDGASLPVGSTHPPSHPPAATD*AA*ANVTDN*NANLV*G   347

Crayfish 3  KKQDGEMESNQINSKKQDGAAAMEMQPLKSAEGGEADEEEEKKVNRPKKE   379
Human 3a    *Q***A***S*TKA******V**************ME*R*K**A*A****   356
Tilapia 2   *M***N******KV***********************K*R***SA****   365
Bullfrog 2a *M***NVDTI*NKA*Q******************DG*DKDK****PH***   397

Crayfish 3  KSVLQGKLTKLAVQIGKAGLVMSAITVIILVLYFVIETFVVEGRPW----   425
Human 3a    ***********************************************T*LAEC   406
Tilapia 2   ********************L*************A*DN***Q****MPEC   415
Bullfrog 2a ********************L******I******A*DN**MQ****MPEC   447
                                        TM3

Crayfish 3  TPVYIQYFVKFFIIGVTVLVVAVPEGLPLAVTISLAYSVKKMMKDNNLVR   475
Human a     **************************************************   474
Tilapia 2   **I***********************************************   465
Bullfrog 2a **I***********************************************   497
                            TM4

Crayfish 3  HLDACETMGNATAICSDKTGTLTTNRMTVVQSYIGDEHYKEIPDPGSLPP   525
Human 3a    *********************************L**T******A*SA*T*   524
Tilapia 2   *****************************A**L*V**VR********V***   515
Bullfrog 2a *****************************A**L*V**VR****P***V***   547
                     Phosphorylation

Crayfish 3  KILDLLVNAISINSAYTTKILPPDKEGDLPKQVGNKTECALLGFVLDLKR   575
Human 3a    *******H*******************A**********************   574
Tilapia 2   *S************************G**********G***L**E***   583
Bullfrog 2a *T**V*****A******S*V**AE***G*KR********G**********   494

Crayfish 3  DYQPIRDQIPEESLYKVYTFNSVRKSMSTVVPMRDGGFRIYSKGASEIVL   625
Human 3a    *F**V*E****D*********************R*P*****LF*******L*   624
Tilapia 2   ******N************************IKLP**S**MY*******V*   633
Bullfrog 2a ***AV*AN****K**********A***********KLE**SY*M********I*   544
                                 FITC

Crayfish 3  KKCSQILNRDGELRSFRPRDKDDMVRKVIEPMACDGLRTICIAYRDFVRG   675
Human 3a    ***TN***SN****G***********I*******************YA*   674
Tilapia 2   H***EV**PRV**********E**K**************V*****SSN   683
Bullfrog 2a ******QGG***T*L*****R*E**K*********************SQS   594

Crayfish 3  CAEINQVHFENEPNWDNENNIMSDLTCLAVVGIEDPVRPEVPDAIQKCQR   725
Human 3a    Q----------**D*****EVVG****I**************E**R****   724
Tilapia 2   P----------**********LN***AI**************N*******   733
Bullfrog 2a P----------**********LN****I**************N*******   644

Crayfish 3  AGITVRMVTGANINTARAIASKCGIIQPGEDFLCLEGKEFNRRIRDEKGC   775
Human 3a    *******************A*************************N***E   774
Tilapia 2   *******************I*****H*******ID*********N***E   773
Bullfrog 2a *******************I*****H*******I**********N***E   694
                                    Crayfish PMCA3 Ab peptide

Crayfish 3  IEQERIDKVWPKLRVLARSSPTDKHTLVKGIIDSTTNDQRQVVAVTGDGT   825
Human 3a    ************************************GE************   814
Tilapia 2   V***********************************GE************   814
Bullfrog 2a V**********************************MA*************   744
                                                       FSBA-Site

Crayfish 3  NDGPALKKADVGFAMGIAGTDVAKEASDIILTDDNFTSIVKAVMWGRNVY   875
Human 3a    **************************************************   864
Tilapia 2   ************************************S*************   873
Bullfrog 2a ************************************S*************   794

Crayfish 3  DSISKFLQFQLTVNVVAVIVAFTGACITQDSPLKAVQMLWVNLIMDTFAS   925
Human 3a    **************************************************   914
Tilapia 2   **************************************************   932
Bullfrog 2  **************************************************   844
                                 TM5               TM6

Crayfish 3  LALATEPPTESLLLRKPYGRTKPLISRTMMKNILGHAVYQLLIIFTLLFV   975
Human 3a    ********************D********************A********   964
Tilapia 2   *************K******N*****S**T******G*************   982
Bullfrog 2a *************K******N*****S**T******G*************   894
                                                TM7

Crayfish 3  GEGFFDIDSGRNAPLHSPPSEHYTIIFNTFVMMQLFNEINARKTHGERNV  1025
Human 3a    **L*****************************************I******  1014
Tilapia 2   **Q***********************************************  1032
Bullfrog 2a **Q*****************************************I******   944
                                             TM8

Crayfish 3  FDGIFSNPIFCTIVLGTFGIQIVIVQFGGKPFSCTPLPAEQWLWCLFVGA  1075
Human 3a    ***************************************S**ST**********V  1064
Tilapia 2   *****R*****S**F***AV**************Q**DL*K*M******L  1082
Bullfrog 2a *****R*****S**F***AV**************Q**DL*K*M******L   994
                  TM9

Crayfish 3  GELVWGQVMATIPTSQLKSLKGAGHEHRKDEMNAEDLNEGQEEIDHAERE  1125
Human 3a    ********I*********C**E***GPG****TD*E*A**E**********  1114
Tilapia 2   *************N*R**F*RR**QLTQ***LPE**V**EN**********  1132
Bullfrog 2a ********I*S***KR**F*****RLTQ*E*NQE*EM**DN**********  1044
                TM10

Crayfish 3  LRRGQILWFRGLNRIQTQIEVVNAFKSGSSVQGAVRRPSSILSQNQDVTN  1175
Human 3a    ******************M***ST**RSG***********V***LH****  1153
Tilapia 2   ******-                                            1112
Bullfrog 2a ***********************T****A*F***L*****TT********  1083
             CaM binding Site

Crayfish 3  VSTPSHG.                                           1182
Human 3a    L***T*AILSAANPTSAAGNPGGESVP.                       1180
Bullfrog 2a **S***VSLSNALSSPTSASAAAAGQG.                       1227
```

Hwang, C.-J. Huang and P. P. Hwang, direct submission to GenBank in 2000, no corresponding publication) and two sequences (*PMCA1bx* and *PMCA2av*) from an amphibian (*Rana catesbiana*, the bullfrog; AF337955 and AF337956, respectively; R. A. Dumont, U. Lins, A. G. Filoteo, J. Penniston, B. Kachar and P. G. Gillespie, direct submissions to GenBank in 2001), all other *PMCA* sequences in GenBank originate in mammalian species.

The crayfish *PMCA3* shares sequence homology with a range of other published *PMCA*s. A phylogenetic tree showing the relationship between the crayfish *PMCA3* amino acid sequence and other *PMCA* sequences available for a diversity of species is provided (Fig. 6). When the *PMCA1–4* protein isoforms were compared, the homology of the same isoform from different species was higher than the similarity between isoforms within a species (Fig. 6). Thus, the crayfish PMCA3 deduced amino acid sequence shared higher identity with mammalian PMCA3 than with PMCA2 from lower vertebrates. Comparing sequence distances within each isoform group (PMCA1 and PMCA2), the sequence distance was always greater between mammalian and non-mammalian species than the distance between species among mammalian or among non-mammalian. The same was true when crayfish PMCA3 was added to the PMCA3 isoform group (Fig. 6). This suggests that *PMCA* genes diverged and their protein products developed specialized functions early in evolution. Regions of sequence difference included the first IC loop between TM2–3 (the 'transduction' domain) and regions in the C-terminus after the CaM binding site that are regulatory sites for various kinases and proteases. The major differences between the deduced crayfish PMCA3 amino acid sequence and other PMCA3 sequences occur in regions close to the sites where alternative splicing originates. Regions that are predictably highly conserved are those that are critical to the catalytic and transport functions of the pump. Several of these regions are located in the large catalytic domain between TM4 and TM5 (phosphorylation site, FITC site, FSBA site, CaM binding site and TM1, 2, 4, 5, 6 and 8). Certain regions where crayfish antennal gland PMCA3 bore a closer resemblance to mammalian PMCA3 than to lower vertebrate PMCA2 (such as TM3 and TM9) presumably differentiate the two isoforms. The regions of high diversity between isoforms are likely to reflect isoform-specific regulatory and functional specializations that allow each pump to fulfill a unique role in the specific cell or

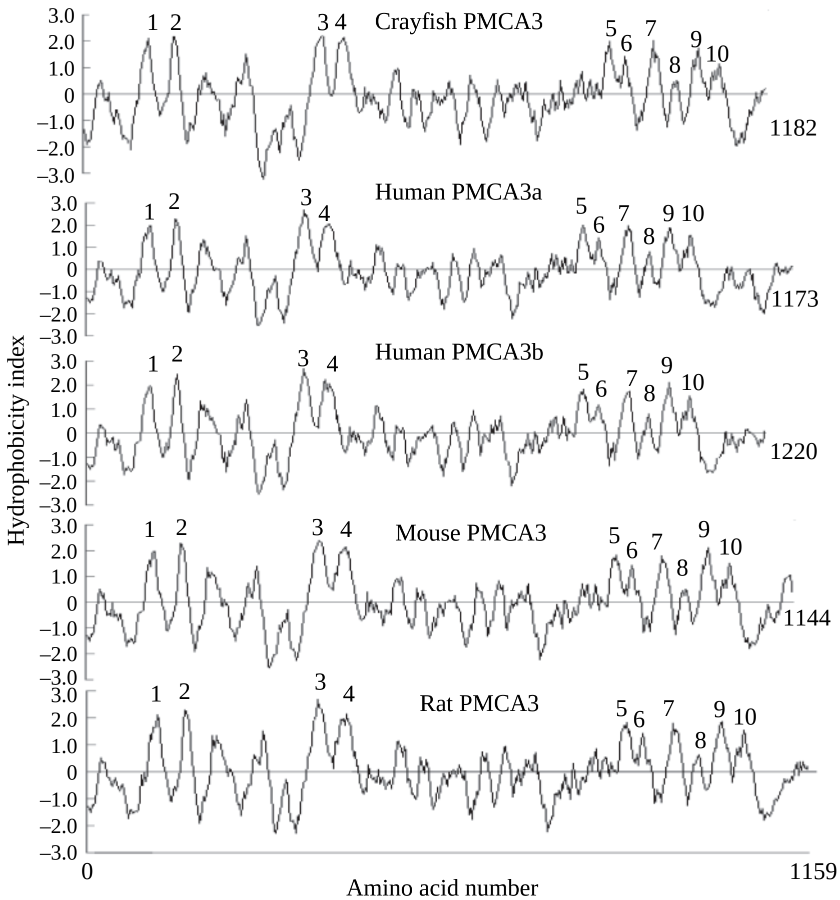

Fig. 2. Hydropathy plot of crayfish antennal gland plasma membrane Ca^{2+}-ATPase (PMCA3) in comparison with that of human PMCA3a (U57931), human PMCA3b (U60414), mouse PMCA3 (AKO32322) and rat PMCA3 (J05087). Hydrophobicity values were determined by the method of Kyte and Doolittle (1982) using a window of 19 residues (http://arbl.cvmbs.colostate.edu/molkit/hydropathy/index.html). Putative transmembrane segments are indicated by the numbers 1–10.

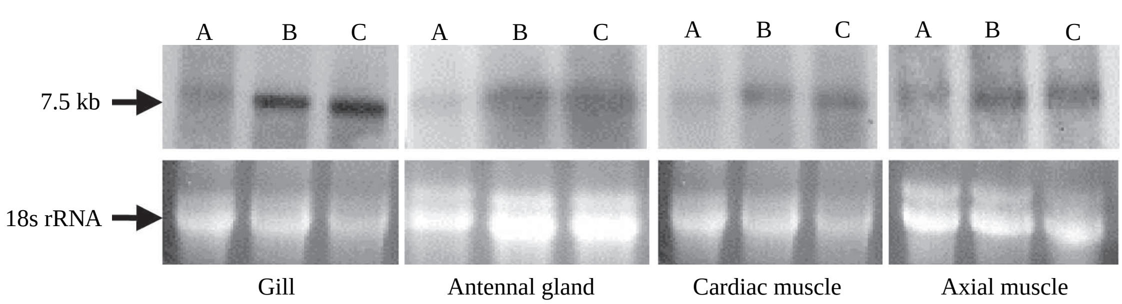

Fig. 3. (Top) Northern blot analysis of plasma membrane Ca^{2+}-ATPase (*PMCA3*) in various crayfish tissues in intermolt (A), premolt (B) and postmolt (C). Total RNA (20 μg) from gill, antennal gland, cardiac muscle and axial abdominal muscle was loaded in each lane. The membrane was hybridized to a 1164 bp crayfish *PMCA3* probe and exposed to X-ray film for 24 h. (Bottom) To normalize the hybridization signal, 18s rRNA concentration was run on a corresponding formaldehyde–agarose gel and visualized by ethidium bromide staining under UV light before being transferred to the membrane. The band size is indicated to the left.

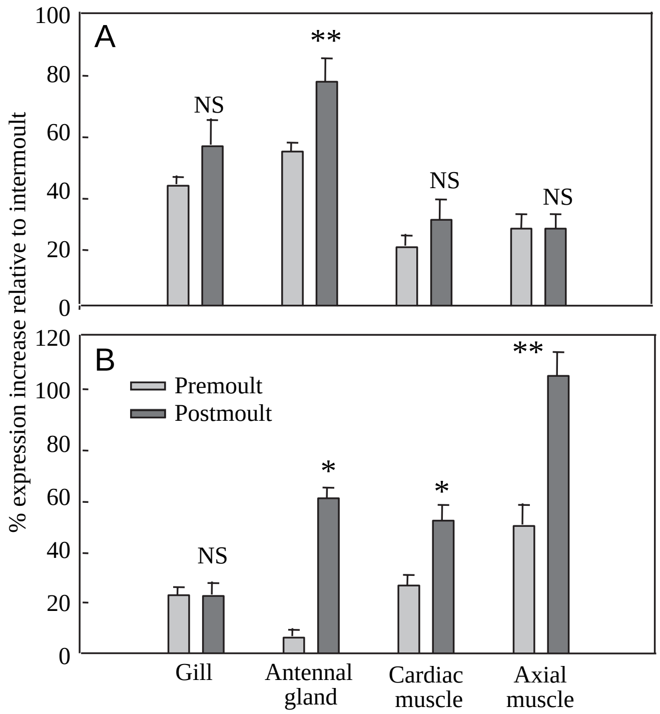

Fig. 4. Quantification of *PMCA3* mRNA (A) and PMCA3 protein (B) from gill, antennal gland, cardiac muscle and axial muscle during molt stages. Values indicate the percentage expression difference compared with the intermolt (control values). Values were obtained from three different scanned X-ray film images and analyzed using KODAK 1D image analysis software. Values are means ± S.E.M. (N=3). All values, except premolt antennal gland, were significantly different (P<0.001) from their intermolt values. Statistical comparison (t-test) between postmolt and premolt expression is indicated as either not significant (NS, P>0.05) or significant (*P<0.01; **P<0.001).

tissue in which it is expressed. Regions where there is high diversity among the same isoforms from different species (TM7 and TM10) are presumably less critical to the function of either isoform. Hydropathy analysis of the crayfish PMCA3 suggested common structural membrane topography to PMCAs described in other species (Strehler, 1991; Monteith and Roufogalis, 1995).

A probe to the novel *PMCA3* crayfish gene hybridized with a single band of 7.5 kb in all tissues tested, suggesting that it is ubiquitously expressed in intermolt at approximately comparable levels. The mRNA species detected in crayfish is the same size as reported in human erythrocyte (Strehler et al., 1990) and rat brain and skeletal muscle (Greeb and Shull, 1989). It is considerably longer than the cDNA sequence represented in Fig. 1A, indicating the presence of an extended untranslated sequence.

The ubiquitous distribution of *PMCA3* in crayfish tissue appears to be in contrast to the tissue distribution in mammals, where it has been restricted primarily to excitable tissues (brain and skeletal muscle – Greeb and Shull, 1989; Burk and Shull, 1992; Carafoli and Stauffer, 1994; Stauffer et al., 1995; hair cells – Furuta et al., 1998). It has also been found at lower levels in regions of the mammalian digestive system and in testis. In mammals, the predominant *PMCA* isoform in transporting epithelia (uterus, liver, kidney and lactating mammary glands) appears to be *PMCA*2 (Stauffer et al., 1997; Furuta et al., 1998; Street et al., 1998; Reinhardt and Horst, 1999). *PMCA3* mRNA expression increased in both premolt and postmolt stages compared with intermolt (Fig. 3) in all crayfish tissues examined irrespective of their involvement in net vectorial Ca^{2+} influx (gill, antennal gland) or not (control tissues, muscle); however, increases were numerically greater in Ca^{2+}-transporting epithelia than in non-Ca^{2+}-transporting tissues, partially supporting the hypothesis on which this study was based. These data support transcriptional regulation of *PMCA* during pre- and postmolt compared with intermolt. The upregulation of *PMCA3* mRNA in premolt antennal gland was greater than observed in gill and increased significantly in postmolt, confirming an earlier prediction from organismal studies (Wheatly et al., 1999) that postmolt Ca^{2+} influx at the antennal gland would necessitate proliferation of Ca^{2+} pumps while gills were engineered with an overcapacity to pump Ca^{2+} in postmolt. Our findings in crayfish confirm an earlier study using semi-quantitative RT-PCR that showed increased expression of PMCA from the non-Ca^{2+}-transporting stages (early premolt) to the stages of $CaCO_3$ deposition/degradation (late premolt/intramolt) in the sternal epithelia of the isopod *Porcellio scaber* (Ziegler et al., 2002). Collectively, both studies would suggest that PMCA plays a role in the vectorial epithelial Ca^{2+} transport.

Antibody raised against crayfish PMCA3 recognized a protein of 128–130 kDa in crayfish tissues, which was the same size as reported in mammalian species (Strehler et al., 1990; Carafoli et al., 1996). Importantly, the protein expression

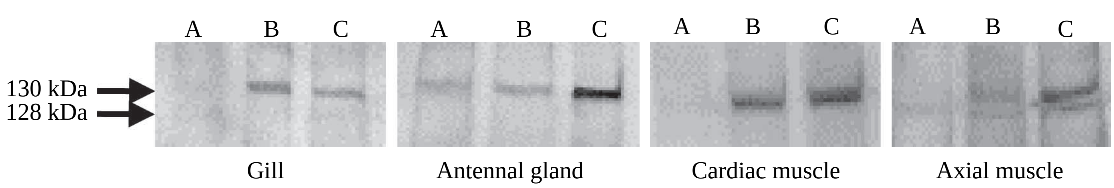

Fig. 5. Western blot analysis of plasma membrane Ca^{2+}-ATPase (PMCA3) in various crayfish tissues in intermolt (A), premolt (B) and postmolt (C). Total plasma membrane protein (30 μg) from gill, antennal gland, cardiac muscle and axial abdominal muscle was loaded in each lane. The membrane was hybridized to a polyclonal antibody (designed against amino acid residues 751–775 EGKEFNRRVRDESGGC of crayfish antennal gland PMCA3 deduced protein sequence; see Fig. 1A for location) and exposed to X-ray film for 2 min.

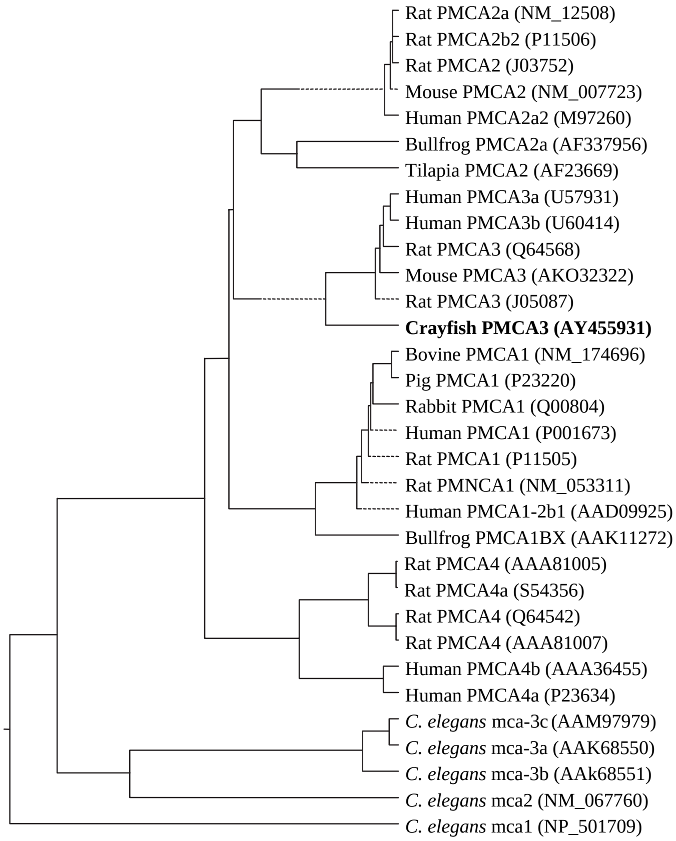

Fig. 6. Phylogram comparison of crayfish PMCA3 amino acid sequence with PMCAs from a diversity of species that are available in GenBank (accession numbers are provided in parentheses). Phylogram values were determined by the Clustal method (DNASTAR, Madison, WI, USA).

patterns (Figs 4B, 5) generally confirmed the mRNA expression patterns described above (Fig. 3), namely that the PMCA3 protein was expressed in all tissues and that expression increased in pre- and postmolt in all tissues examined compared with intermolt. For gill and antennal gland, protein expression patterns paralleled those observed for mRNA, indicating that *PMCA3* was transcriptionally regulated. In muscle, however, protein expression increased in postmolt compared with premolt even though mRNA expression had been unchanged. The best available explanation would be that rate of mRNA translation was increased or that the appearance of a second protein band confounded the image analysis.

The expression pattern observed for *PMCA3* during the molting cycle directly opposes the pattern previously reported for SERCA, the Ca^{2+} pump located on endomembranes. In both epithelial (hepatopancreas) and non-epithelial tissues (muscle), SERCA expression was highest in intermolt and decreased in both pre- and postmolt to expression levels that were roughly comparable (Zhang et al., 2000; Chen et al., 2002). Thus, in crayfish non-mineralizing tissues, PMCA and SERCA expression patterns seem to be inversely regulated during molting stages. Overexpression of *PMCA* in rat aortic endothelial cells similarly resulted in downregulation of SERCA (Liu et al., 1996). It has been suggested that the genes for all the major Ca^{2+}-transporting pathways are linked for regulatory purposes.

Interestingly, in an arthropod mineralizing tissue, the anterior sternal epithelium of the isopod *Porcellio scaber* (Hagedorn et al., 2003), an increase in SERCA expression was observed from the non-transporting early premolt stage to the Ca^{2+}-transporting late premolt and intramolt stage. These changes were not seen in nervous tissue. This would suggest a role for SERCA in transcellular Ca^{2+} transport in mineralization processes. Related studies revealed that IC Ca^{2+} hotspots represent SER cisternae (Ziegler, 2002) and that SERCA activity increased by fivefold from early premolt to the Ca^{2+}-transporting late premolt and intramolt (Hagedorn and Zeigler, 2002). Similarly, SERCA activity has been shown to increase in rat dental ameloblasts during calcification. Mineralizing tissues display Ca^{2+} flux rates that are much higher than other Ca^{2+}-transporting epithelia (such as kidney) and it seems plausible that they may have evolved routes for Ca^{2+} transit that exceed typical transepithelial rates. Seemingly, there are differences in expression of Ca^{2+} import/export proteins between mineralizing and non-mineralizing tissues that warrant further investigation.

The Ca^{2+} secretory model of pregnant and lactating rats revealed that five different Ca^{2+} pumps in mammary tissue (PMCA1b, 2b and 4b and SERCA2 and 3) were all upregulated by the 14th day of lactation (Reinhardt and Horst, 1999). In this model, a large amount of Ca^{2+} moves across the cell from the blood to the milk. In this case, PMCA and SERCA trends were the same, suggesting that the lactating mammary gland model has more in common with the isopod mineralizing model.

Since PMCA3 has such a restrictive tissue-specific distribution in mammals (primarily neuronal/excitable) there are relatively few studies that have examined regulation of expression, particularly in response to Ca^{2+} flux. However, evidence is accumulating that regulation of Ca^{2+}-associated genes is centrally regulated by changes in IC Ca^{2+} itself (Zacharias and Strehler, 1996; Kuo et al., 1997; Carafoli et al., 1999; Guerini et al., 1999). For example, rat cerebellar granule cells kept under depolarizing conditions for several days (leading to increased Ca^{2+} influx) showed a marked upregulation of PMCA3 at both the mRNA and protein levels (also of PMCA1a and PMCA2; Guerini et al., 1999). Functionally, the PMCAs appear to play an important role in cellular Ca^{2+} dynamics. A number of different regulatory mechanisms may alter their functionality (Carafoli, 1991; Monteith and Roufogalis, 1995; Penniston and Enyedi, 1998). Primarily, PMCAs are activated by Ca^{2+}-calmodulin, acidic phospholipids and serine/threonine phosphorylation (James et al., 1988; Enyedi et al., 1989; Falchetto et al., 1991, 1992). In addition to mediating regulation by Ca^{2+}-calmodulin, the COOH-terminal region of the calcium pump has also been shown to be the target of phosphorylation by protein kinases A and C (Wuytack et al., 1992; Monteith and

Roufogalis, 1995; Penniston and Enyedi, 1998) and to be affected by proteases such as calpain (Carafoli, 1994; Wang et al., 1994).

The present study has cloned and sequenced the entire *PMCA3* from the crayfish *Procambarus clarkii*. Sequence data will inform our general understanding of the molecular evolution of this important *PMCA* isoform. Expression of PMCA3 mRNA and protein increased in all tissues examined in the pre- and postmolt stage, a period during which Ca^{2+} influx at transporting epithelia contributes to overall Ca^{2+} conservation as the organism seeks to remineralize its cuticle. As we seek to more fully understand the regulation of PMCA and other Ca^{2+}-associated membrane proteins (SERCAs, Ca^{2+} channels and NCX), the crustacean molting cycle will continue to offer an interesting non-mammalian model.

The *PMCA3* sequence from the crayfish *Procambarus clarkii* antennal gland has been accepted by GenBank (accession no. AY455931).

This work was supported by National Science Foundation Grant IBN 0076035 to M.G.W.

References

Altschul, S. F., Gish, W., Miller, W., Myers, E. W. and Lipman, D. J. (1990). Basic local alignment search tool. *J. Mol. Biol*. **215**, 403-410.

Axelsen, K. B. and Palmgren, M. G. (1998). Evolution of substrate specificities in the P-type ATPase superfamily. *J. Mol. Evol.* **46**, 84-101.

Boersma, W. J. A., Haaijman, J. J. and Claassen, E. (1993). Use of synthetic peptide determinants for the production of antibodies. In *Immunohistochemistry*, vol. II (ed. A. C. Cuello), pp. 1-78. New York: Wiley.

Borke, J. L., Caride, A., Verma, A. K., Penniston, J. T. and Kumar, R. (1990). Cellular and segmental distribution of Ca^{2+}-pump epitopes in rat intestine. *Eur. J. Physiol*. **417**, 120-122.

Bourinet, E., Soong, T. W., Sutton, K., Slaymaker, S., Mathews, E., Monteil, A., Zamponi, G. W., Nargeot, J. and Snutch, T. P. (1999). Splicing of α 1A subunit gene generates phenotypic variants of P- and Q-type calcium channels. *Nature Neurosci.* **2**, 407-415.

Brandt, P., Neve, R. L., Kammesheidt, A., Rhoads, R. E. and Vanaman, T. C. (1992). Analysis of the tissue-specific distribution of mRNAs encoding the plasma membrane calcium-pumping ATPases and characterization of the alternately spliced form of PMCA4 at the cDNA and genomic levels. *J. Biol. Chem.* **267**, 4376-4385.

Brown, B. J., Hilfiker, H., DeMarco, S. J., Zacharias, D. A., Greenwood, T. M., Guerini, D. and Strehler, E. E. (1996). Primary structure of human plasma membrane $Ca^{(2+)}$-ATPase isoform 3. *Biochim. Biophys. Acta* **1283**, 10-13.

Burk, S. E. and Shull, G. E. (1992). Structure of the rat plasma membrane Ca^{2+}-ATPase isoform 3 gene and characterization of alternative splicing and transcription products. *J. Biol. Chem.* **267**, 19683-19690.

Carafoli, E. (1991). Calcium pump of the plasma membrane. *Physiol. Rev*. **71**, 129-153.

Carafoli E. (1994). Biogenesis, plasma membrane calcium ATPase, 15 years of work on the purified enzyme. *FASEB. J.* **8**, 993-1002.

Carafoli, E., Garcia-Martin, E. and Guerini, D. (1996). The plasma membrane calcium pump, recent developments and future perspectives. *Experientia* **52**, 1091-1100.

Carafoli, E., Genazzani, A. and Guerini, D. (1999). Calcium controls the transcription of its own transporters and channels in developing neurons. *Biochem. Biophys. Res. Commun.* **266**, 624-632.

Carafoli, E. and Stauffer, T. (1994). The plasma membrane calcium pump, functional domains, regulation of the activity, and tissue specificity of isoform expression. *J. Neurobiol.* **25**, 312-324.

Carninci, P., Shibata, Y., Hayatsu, N., Sugahara, Y., Shibata, K., Itoh, M., Konno, H., Okazaki, Y., Muramatsu, M. and Hayashizaki, Y. (2000). Normalization and subtraction of cap-trapper-selected cDNAs to prepare full-length cDNA libraries for rapid discovery of new genes. *Genome Res.* **10**, 1617-1630.

Chen, D., Zhang, Z., Wheatly, M. G. and Gao, Y. (2002). Cloning and characterization of the heart muscle isoform of sarco/endoplasmic reticulum Ca^{2+} ATPase (SERCA) from crayfish. *J. Exp. Biol*. **205**, 2677-2686.

De Jaegere, S., Wuytack, F., Eggermont, J. A., Verboomen, H. and Casteels, R. (1990). Molecular cloning and sequencing of the plasma-membrane Ca^{2+} pump of pig smooth muscle. *Biochem. J.* **271**, 655-660.

Enyedi, A., Vorherr, T., James, P., McCormick, D. J., Filoteo, A. G., Carafoli, E. and Penniston, J. T. (1989). The calmodulin binding domain of the plasma membrane Ca^{2+} pump interacts both with calmodulin and with another part of the pump. *J. Biol. Chem.* **264**, 12313-12321.

Falchetto, R., Vorherr, T., Brunner, J. and Carafoli, E. (1991). The plasma membrane Ca^{2+} pump contains a site that interacts with its calmodulin-binding domain. *J. Biol. Chem*. **266**, 2930-2936.

Falchetto, R., Vorherr, T. and Carafoli, E. (1992). The calmodulin binding site of the plasma membrane Ca^{2+} pump interacts with the transduction domain of the enzyme. *Protein Sci.* **1**, 1612-1621.

Furuta, H., Luo, L., Hepler, K. and Ryan, A. F. (1998). Evidence for differential regulation of calcium by outer versus inner hair cells, plasma membrane Ca-ATPase gene expression. *Hear. Res.* **123**, 10-26.

Greeb, J. and Shull, G. E. (1989). Molecular cloning of a third isoform of the calmodulin-sensitive plasma membrane Ca^{2+}-transporting ATPase that is expressed predominantly in brain and skeletal muscle. *J. Biol. Chem*. **264**, 18569-18576.

Guerini, D., Garcia-Martin, E., Gerber, A., Volbracht, C., Leist, M., Gutierrez Merino, C. and Carafoli, E. (1999). The expression of plasma membrane Ca^{2+} pump isoforms in cerebellar granule neurons is modulated by Ca^{2+}. *J. Biol. Chem*. **274**, 1667-1676.

Guerini, D., Wang, X., Li, L., Genazzani, A. and Carafoli, E. (2000). Calcineurin controls the expression of isoform 4CII of the plasma membrane Ca^{2+} pump in neurons. *J. Biol. Chem.* **275**, 3706-3712.

Hagedorn, M., Weihrauch, D., Towle, D. W. and Ziegler, A. (2003). Molecular characterisation of the smooth endoplasmic reticulum Ca^{2+} –ATPase of *Porcellio scaber* and its expression in sternal epithelia during the moult cycle. *J. Exp. Biol.* **206**, 2167-2175.

Hagedorn, M. and Ziegler, A. (2002). Analysis of Ca^{2+} uptake into the smooth endoplasmic reticulum of permeabilised sternal epithelial cells during the moulting cycle of the terrestrial isopod *Porcellio scaber*. *J. Exp. Biol.* **205**, 1935-1942.

Hilfiker, H., Strehler-Page, M. A., Stauffer, T. P., Carafoli, E. and Strehler, E. E. (1993). Structure of the gene encoding the human plasma membrane calcium pump isoform 1. *J. Biol. Chem.* **268**, 19717-19725.

Howard, A., Barley, N. F., Legon, S. and Walters, R. F. (1994). Plasma-membrane calcium-pump isoforms in human and rat liver. *Biochem. J.* **303**, 275-279.

James, P., Maeda, M., Fischer, R., Verma, A. K., Krebs, J., Penniston, J. T. and Carafoli, E. (1988). Identification and primary structure of a calmodulin binding domain of the Ca^{2+} pump of human erythrocytes. *J. Biol. Chem.* **263**, 2905-2910.

Kamath, R. S., Fraser, A. G., Dong, Y., Poulin, G., Durbin, R., Gotta, M., Kanapin, A., Le Bot, N., Moreno, S., Sohrmann, M. et al. (2003). Systematic functional analysis of the *Caenorhabditis elegans* genome using RNAi. *Nature* **421**, 231-237.

Keeton, T. P. and Shull, G. E. (1995). Primary structure of rat plasma membrane Ca^{2+}-ATPase isoform 4 and analysis of alternative splicing patterns at splice site A. *Biochem. J.* **306**, 779-785.

Kraev, A., Kraev, N. and Carafoli, E. (1999). Identification and functional expression of the plasma membrane calcium ATPase gene family from *Caenorhabditis elegans. J. Biol. Chem.* **274**, 4254-4258.

Krizaj, D., Demarco, S. J., Johnson, J., Strehler, E. E. and Copenhagen, D. R. (2002). Cell-specific expression of plasma membrane calcium ATPase isoforms in retinal neurons. *J. Comp. Neurol.* **451**, 1-21.

Kuo, T. H., Liu, B. F., Yu, Y., Wuytack, F., Raeymaekers, L. and Tsang, W. (1997). Co-ordinated regulation of the plasma membrane calcium pump and the sarco(endo)plasmic reticular calcium pump gene expression by Ca^{2+}. *Cell Calcium* **21**, 399-408.

Kuzmin, I., Stackhouse, T., Latif, F., Duh, F. M., Geil, L., Gnarra, J., Yao, M., Li, H., Tory, K., Le Paslier, D. et al. (1994). One-megabase yeast artificial chromosome and 400-kilobase cosmid-phage contigs containing the von Hippel-Lindau tumor suppressor and Ca^{2+}-transporting adenosine triphosphatase isoform 2 genes. *Cancer Res.* **54**, 2486-2491.

Kyte, J. and Doolittle, R. F. (1982). A simple method for displaying hydropathic character of a protein. *J. Mol. Biol.* **157**, 105-132.

Latif, F., Duh, F. M., Gnarra, J., Tory, K., Kuzmin, I., Yao, M., Stackhouse, T., Modi, W., Geil, L., Schmidt, L. et al. (1993). Von Hippel-Lindau syndrome, cloning and identification of the plasma membrane Ca^{2+}-transporting ATPase isoform 2 gene that resides in the Von Hippel-Lindau gene region. *Cancer Res*. **53**, 861-867.

Lehotsky, J. (1995). Plasma membrane Ca^{2+}-pump functional specialization in the brain. Complex of isoform expression and regulation by effectors. *Mol. Chem. Neuropathol*. **25**, 175-187.

Liu, B. F., Xu, X., Fridman, R., Muallem, S. and Kuo, T. H. (1996). Consequences of functional expression of the plasma membrane Ca^{2+} pump isoform 1a. *J. Biol. Chem.* **271**, 5536-5544.

Lutsenko, S. and Kaplan, J. H. (1995). Organization of P-type ATPases, significance of structural diversity. *Biochemistry* **34**, 15608-15613.

McWhinnie, M. (1962). Gastrolith growth and calcium shifts in the freshwater crayfish *Orconectes virilis. Comp. Biochem. Physiol*. **7**, 1-14.

Monteith, G. R. and Roufogalis, B. D. (1995). The plasma membrane calcium pump, a physiological perspective on its regulation. *Cell Calcium* **18**, 459-470.

Olson, S., Wang, M. G., Carafoli, E., Strehler, E. E. and McBride, O. W. (1991). Localization of two genes encoding plasma membrane Ca^{2+} transporting ATPases to human chromosomes 1q25-32 and 12q21-23. *Genomics* **9**, 629-641.

Penniston, J. T. and Enyedi, A. (1998). Modulation of the plasma membrane Ca^{2+} pump. *J. Membr. Biol.* **165**, 101-109.

Reinhardt, T. A. and Horst, R. L. (1999). Ca^{2+}-ATPases and their expression in the mammary gland of pregnant and lactating rats. *Am. J. Physiol.* **276**, C796-C802.

Schatzmann, H. J. (1966). ATP-dependent Ca^{++} extrusion from human red cells. *Experientia* **22**, 364-368.

Shull, G. E. and Greeb, J. (1988). Molecular cloning of two isoforms of the plasma membrane Ca^{2+}-transporting ATPase from rat brain. *J. Biol. Chem.* **263**, 8646-8657.

Stauffer, T. P., Hilfiker, H., Carafoli, E. and Strehler, E. E. (1993). Quantitative analysis of alternative splicing options of human plasma membrane calcium pump genes. *J. Biol. Chem.* **268**, 25993-26003.

Stauffer, T. P., Guerini, D. and Carafoli, E. (1995). Tissue distribution of the four gene products of the plasma membrane Ca^{2+} pump. A study using specific antibodies. *J. Biol. Chem.* **270**, 12184-12190.

Stauffer, T. P., Guerini, D., Celio, M. R. and Carafoli, E. (1997). Immunolocalization of the plasma membrane Ca^{2+} pump isoforms in the rat brain. *Brain Res*. **748**, 21-29.

Street, V. A., McKee-Johnson, J. W., Fonseca, R. C., Tempel, B. L. and Noben-Trauth, K. (1998). Mutations in a plasma membrane Ca^{2+}-ATPase gene cause deafness in deafwaddler mice. *Nature Genet.* **19**, 390-394.

Strehler, E. E. (1991). Recent advances in the molecular characterization of plasma membrane Ca^{2+} pumps. *J. Membr. Biol.* **120**, 1-15.

Strehler, E. E., James, P., Fischer, R., Heim, R., Vorherr, T., Filoteo, A. G., Penniston, J. T. and Carafoli, E. (1990). Peptide sequence analysis and molecular cloning reveal two calcium pump isoforms in the human erythrocyte membrane. *J. Biol. Chem.* **265**, 2835-2842.

Verma, A. K., Filoteo, A. G., Stanford, D. R., Wieben, E. D., Penniston, J. T., Strehler, E. E., Fisher, R., Heim, R., Vogel, G., Salima, M. et al. (1988). Complete primary structure of a human plasma membrane Ca^{2+} pump. *J. Biol. Chem.* **263**, 14152-14159.

Wang, M. G., Yi, H., Hilfiker, H., Carafoli, E., Strehler, E. E. and McBride, O. W. (1994). Localization of two genes encoding plasma membrane Ca^{2+} ATPases isoform 2 (ATP2B2) and 3 (ATP2B3) to human chromosomes 3p26→p25 and Xq28, respectively. *Cytogenet. Cell. Genet*. **67**, 41-45.

Waterston, R. (1998). Genome sequence of the nematode *C. elegans*, a platform for investigating biology. The *C. elegans* Sequencing Consortium. *Science* **282**, 2012-2018.

Wheatly, M. G. (1999). Calcium homeostasis in Crustacea, the evolving role of branchial, renal, digestive and hypodermal epithelia. *J. Exp. Zool*. **283**, 277-284.

Wheatly, M. G., Pence. R. C. and Weil, J. R. (1999). ATP-dependent calcium uptake into basolateral vesicles from transporting epithelia of intermolt crayfish. *Am. J. Physiol* **276**, R566-R574.

Wheatly, M. G., Zhang, Z., Weil, J. R., Rogers, J. V. and Stiner, L. M. (2001). Novel subcellular and molecular tools to study Ca transport mechanisms during the elusive moulting stages of crustaceans, flow cytometry and polyclonal antibodies. *J. Exp. Biol.* **204**, 959-966.

Williams, J. R., Sharp, J. W., Kumari, V. G., Wilson, M. and Payne, J. A. (1999). The neuron-specific K-Cl cotransporter, KCC2, antibody development and initial characterization of the protein. *J. Biol. Chem.* **274**, 12656-12664.

Wuytack, F., Raeymaekers, L., De Smedt, H., Eggermont, J. A., Missiaen, L., Van Den Bosch, L., De Jaegere, S., Verboomen, H. and Plessers, L. and Casteel, R. (1992). Ca^{2+}-transport ATPases and their regulation in muscle. *Ann. New York Acad. Sci.* **671**, 82-91.

Zacharias, D. A. and Kappen, C. (1999). Developmental expression of the four plasma membrane calcium ATPase (*PMCA*) genes in the mouse. *Biochim. Biophys. Acta.* **1428**, 397-405.

Zacharias, D. A. and Strehler, E. E. (1996). Change in plasma membrane Ca^{2+}-ATPase splice-variant expression in response to a rise in intracellular Ca^{2+}. *Curr. Biol.* **6**, 1642-1652.

Zacharias, D. A., Dalrymple, S. J. and Strehler, E. E. (1995). Transcript distribution of plasma membrane Ca^{2+} pump isoforms and splice variants in the human brain. *Mol. Brain. Res.* **28**, 263-272.

Zhang, Z., Chen, D. and Wheatly, M. G. (2000). Cloning and characterization of sarco/endoplasmic reticulum $Ca^{(2+)}$-ATPase (SERCA) from crayfish axial muscle. *J. Exp. Biol.* **22**, 3411-3423.

Ziegler, A. (2002). X-ray microprobe analysis of epithelial calcium transport. *Cell Calcium* **31**, 307-321.

Ziegler, A., Weihrauch, D., Towle, D. W. and Hagedorn, M. (2002). Expression of Ca^{2+} ATPase and Na/Ca exchanger is upregulated during epithelial Ca^{2+} transport in hypodermal cells of the isopod *Porcellio scaber*. *Cell Calcium* **32**, 131-141.